Mutation Effects on FAS1 Domain 4 Related to Protein Aggregation by Molecular Dynamics Simulations and Solvation Free Energy Analysis

Sunhee Cho and Sihyun Ham*

Department of Chemistry, Sookmyung Women's University,
Hyochangwon-gil 52, Yongsan-gu, Seoul, 140-742, Korea.
E-mail: sihyun@sookmyung.ac.kr

Fasciclin 1 (FAS1) is an extracellular protein whose aggregation in cornea leads to visual impairment. While a number of FAS1 mutants have been studied that exhibit enhanced/decreased aggregation propensity, no structural information has been provided so far that is associated with distinct aggregation potential. In this study, we have investigated the structural and thermodynamic characteristics of the wild-type FAS1 and its two mutants, R555Q and R555W, by using molecular dynamics simulations and three-dimensional reference interaction site model (3D-RISM) theory. We find that the hydrophobic solvent accessible surface area increases due to hydrophobic core repacking in the C-terminus caused by the mutation. We also find that the solvation free energy of the mutants increases due to the enhanced non-native H-bonding. These structural and thermodynamic changes upon mutation contribute to understand the aggregation of these mutants.

Key Words : Molecular Dynamics Simulations, Protein Mutation, Protein Aggregation, Corneal Dystrophy, Solvation Free Energy

Introduction

The transforming growth factor-beta induced protein (TGFBIp, also known as βig-h3) gene was first identified in an adenocarcinoma cell line[1]. The TGFBIp is found at various human tissues including the cornea of eyes[2] consists of four domains denoted as fasciclin 1 protein (FAS1) domains. This protein is an extracellular matrix protein mainly found in cornea[2], skin[3], bone[4], and kidney[5] in human. The TGFBIp has a molecular weights of 68-70 kDa in their isoforms after partial cleavage in the C-terminus, and binds to various extracellular matrix components, such as fibronectin, laminin and some collagens.[6,7] A number of previous reports support various functions of the TGFBIp such as wound healing, cell growth, cell differentiation, apoptosis and tumorgenesis, but the biological function remains unclear.[8-10]

At present, over 30 mutations causing different kinds of corneal dystrophy have been identified.[11] Especially R124 and R555, called hot spot, increase/decrease protein aggregation upon its mutation associated with a corneal dystrophy in eyes.[12,13] These two mutation sites are located at solvent-exposed   -helical regions. This may reduce solubility or stability of mutants and it is the possible disease mechanism related to certain corneal dystrophies.[14,15] For example, R555Q mutation forms a protein deposit of curly fibers, whereas the R555W mutant induces fuchsinophilic granular deposits.[11] However the aggregation propensity is unknown. Some papers have been reported that the R555 mutants are non-amyloid proteins[16] but, in the other

hand, R555W mutant is amyloid protein[13]. Nonetheless, a specific mutation of TGFBIp forms a specific type of corneal dystrophy disease, which results in a reduction of visual power and in eventual blindness due to the protein aggregation in the cornea.[16] However, no structural information and unknown aggregation propensity have been provided on the conformational characteristics for these mutants associated with corneal dystrophy.

In this study, we show the structural characterization and thermodynamics for the disease related mutants, R555Q and R555W, of the wild type FAS1 domain 4 protein (wtFAS1) by using all-atom, explicit water molecular dynamics (MD) simulations as well as three-dimensional reference interaction site model (3D-RISM) theory. The aims of this work are three fold. First, it is to determine the structural variations caused by the disease-causing point mutation (R555Q and R555W) with respect to the wtFAS1. Second, it is to provide the molecular motifs for how the different structural features by point mutation would induce different protein-protein interaction to promote the aggregation of wtFAS1. Lastly, it is to elucidate the solvation effect and hydrophobicity changes in relation to the protein aggregation in FAS1.

Theory and Computational Method

1. Molecular Dynamics Simulations

We performed all-atom, explicit-water MD simulations at 360 K and 1 bar on wtFAS1 and its

two mutants (R555Q and R555W) by using SANDER module of AMBER 9[17] package. All production runs were simulated for 50 ns under neutral pH. We employed the ff99SB force field[18] for protein and the TIP3P model[19] for water. The initial conformation was taken from X-ray structure. We used PDB entry 2VXP (Figure 1) for wild-type FAS1 and generated two mutants by simply replacing Alanine 555 into Glutamine (R555Q) and Tryptophan (R555W) based on crystal structure of wtFAS1 by Swiss PDB viewer[20]. Particle mesh Ewald method[21] was applied for treating electrostatic interactions. The SHAKE algorithm[22] was employed for bonds including hydrogen atoms.

2. Solvation Free Energy Analysis

We calculated the three-dimensional reference interaction site model (3D-RISM) theory[23,24] for solvation free energy analysis. The 3D-RISM theory is an integral-equation theory based on statistical mechanics for obtaining the 3D distribution function $g_i(r) = h_i(r) + 1$ of the water *site i* at position *r* around a protein. In this theory, the 3D-RISM equation

$$h_i(\mathbf{r}) = \sum_j \int d\mathbf{r}' \chi_{ij}(|\mathbf{r} - \mathbf{r}'|) c_j(\mathbf{r}')$$

is solved self-consistently with the closure relation

$$h_i(\mathbf{r}) = \begin{cases} \exp[-\beta u_i(\mathbf{r}) + h_i(\mathbf{r}) - c_i(\mathbf{r})] - 1 & \text{for} \quad h_i(\mathbf{r}) \le 0 \\ -\beta u_i(\mathbf{r}) + h_i(\mathbf{r}) - c_i(\mathbf{r}) & \text{for} \quad h_\gamma(\mathbf{r}) > 0 \end{cases}$$

In these equations, $c_i(\mathbf{r})$ is the direct correlation function, $\chi_{ij}(r)$ is the water susceptibility function, $u_i(\mathbf{r})$ is the protein-water interaction potential, and $\beta = 1/(k_B T)$ is the inverse temperature. The solvation free energy G_{solv} is then obtained from

$$G_{\text{solv}} = \rho k_B T \sum_i \int d\mathbf{r} \left[\frac{1}{2} h_i(\mathbf{r})^2 \Theta(-h_i(\mathbf{r})) - c_i(\mathbf{r}) - \frac{1}{2} h_i(\mathbf{r}) c_i(\mathbf{r}) \right]$$

where ρ is the average number density of water and $\Theta(x)$ is the Heaviside step function.

Results and Discussion

Mutation effects on global structures

To characterize the structural dynamics of wtFAS1 (Figure 1) and its two mutants (R555Q and R555W)

by performing the MD simulations, we first investigated the Cα root-mean-square deviation (RMSD). The Cα RMSD values of wtFAS1 and its two mutants are within a few average value of 2.7 Å (standard deviation: 0.3 Å), 2.5 Å (0.4 Å), and 2.1 Å (0.3 Å) for wtFAS1, R555Q, and R555W, respectively. Secondly, Figure 2 shows the Cα root-mean-square fluctuations (RMSF) of three proteins. The fluctuation regions are helical regions (α4-α5-α6), loop regions (L7, L8, L9, and L10), and β2-β3-β4 regions.
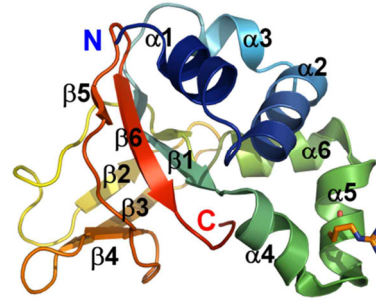

Figure 8. Crystal structure of wild type FAS1 domain 4 protein consists of 131 residues. The color-code starts with blue, N-terminus as follows the order of the amino acid sequence and ends with red, C- terminus. The mutation site, R555, is represented as a stick (C and N: orange and blue)
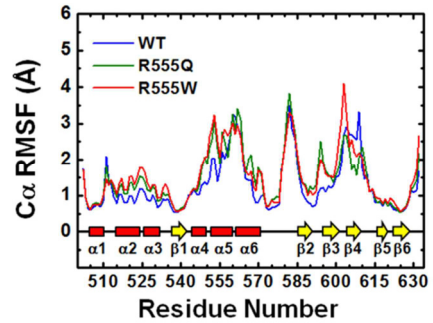
Figure 2. Backbone Cα RMSFs based on residues.

While the global structures of wtFAS1 and its two mutants (R555Q and R555W) are largely maintained during the entire simulation time, the heterogeneities in conformational dynamics are indicated. (Figure 3) Replacing R555 into Gln and Trp is increasing the number of hydrophobic contacts in the order of wtFAS1 (31.3 ± 2.2), R555Q (34.5 ± 1.9), and R555W (36.9 ± 1.7). The α2-α4-α5-α6 region of two mutants is more compact than that of wild type. This is further verified with the results of solvent accessible surface area (SASA).
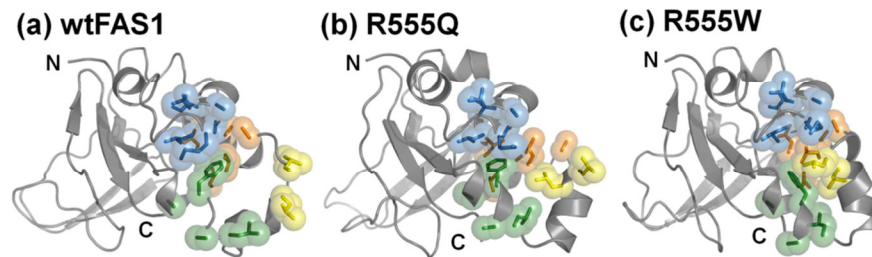
Figure 3. Most representative structures with hydrophobic residues (a) wtFAS1, (b) R555Q, (c) R555W.

The difference of SASA for hydrophobic residues in two mutants is negative value (-153.3 Å^2 for R555Q and -123.6 Å^2 for R555W) compared to that of wtFAS1. This comes from the induced hydrophobic contacts of $\alpha2$-$\alpha4$-$\alpha5$-$\alpha6$ region.

Hydrophobic residues around residue 555 are shown in as stick and sphere representation and depicted with different colors (sky blue: α2, green: α4, yellow: α5, orange: α6). Side-chains, Cα, and Hα atoms are only shown and the others are omitted for clarity.

Replacing positively charged and solvent-exposed Arginine 555 into neutral Glutamine and Tryptophan enhances hydrophobic contacts[13]. Noticeably, by R555 mutations, the relative orientation of $\alpha4$-$\alpha5$-$\alpha6$ helices is rearranged in both mutants. In the case of the R555Q mutation, the side-chain of Q555 forms non-native H-bonding with carbonyl oxygen of L550 backbone and this induces well-organized hydrophobic regions in $\alpha2$-$\alpha4$-$\alpha5$-$\alpha6$ regions. In the case of the R555W mutation, because the Tryptophan residue is hydrophobic, it triggers greater number of hydrophobic contacts in $\alpha2$-$\alpha4$-$\alpha5$-$\alpha6$ regions. As a result, both R555Q and R555W mutants display higher degrees of hydrophobic interactions than that of wtFAS1 around the mutation site in $\alpha2$-$\alpha4$-$\alpha5$-$\alpha6$ region.

YH motif blockage by rearrangement of C-terminus

Although the biological functions of TGFBIp are still unclear, the TGFBIp has been proposed to be related to the cell adhesion by binding with integrins.[8,26-28] A few promising binding sites have been reported as YH motif (Y571 and H572) and DI motif (D617 and I618) and they are fairly conserved

in other FAS1 domains.[29,30] In the case of the DI motif, the binding site is on the interface of FAS1 domain 3. Therefore it would be difficult to bind with integrins without any conformational changes. In contrast with the DI motif, YH motif is located at the $\alpha6$ region which is on the surface. The YH motif is solvent-exposed and can provide potential binding site. Interestingly, introducing point mutation at the residue 555 alters the local conformational features around YH motif. Due to the induced hydrophobic interactions in $\alpha2$-$\alpha4$-$\alpha5$-$\alpha6$ regions of two mutants, the C-terminus is rearranged to be located on the protein surface. As a result, two exposed hydrophobic residues of C-terminus, V631 and L632, block the YH motifs. This happens both in R555Q and R555W mutants. (Figure 4) The blockage of YH motif is also verified with SASA analysis. SASA for YH motif is decreased (-34.3 Å^2 for R555Q and -77.5 Å^2 for R555W), on the other hand, that of C-terminus is increased (53.8 Å^2 for R555Q and 13.7 Å^2 for R555W). This indicates that due to the rearrangement of two C-terminus residues, the YH motif is disturbed. This cause the protein dysfunction which may contribute to promote protein aggregation.

Disruption of $\beta2$-$\beta3$-$\beta4$ regions by non-native H-bonding

Higher degrees of hydrophobic interactions around the mutations site affects not only YH motif but also $\beta2$-$\beta3$-$\beta4$ regions. As shown in Figure 5, large fluctuations were observed. The number of H-bonding of mutants is decreased fairly in $\beta2$-$\beta3$-$\beta4$ regions during the simulation time. On the contrary, in the case of wtFAS1, the number of H-bonding maintains its values, only shows small subtle fluctuations. This may arise because of the rearrangement of C-terminus caused by hydrophobic interactions of $\alpha2$-$\alpha4$-$\alpha5$-$\alpha6$ regions.
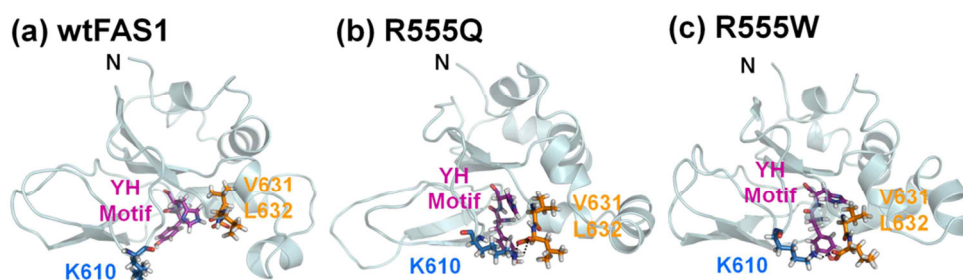
Figure 4. YH binding motifs (Y571 and H572), two hydrophobic residues (V631 and L632) of the C-terminus, and K610 for (a) wtFAS1, (b) R555Q, and (c) R555W are shown as a stick representation. The color of C atom for YH motif is magenta, of C-terminus is orange, and of K610 is blue. The others (N, O, and H) are blue, red, and white, respectively.

Table 1. The difference of solvation free energy ($\Delta\Delta\mu$) of β2-β3-β4 regions in R555Q and R555W with respect to wtFAS1. (unit: kcal/mol)

	Solvation free energy ($\Delta\Delta\mu$)
R555Q	+53.85
R555W	+115.24

Two residues (V631 and L632) of C-terminus located on the protein surface form non-native H-bonding with adjacent hydrophilic residues. In the case of wtFAS1, the C-terminus is located inside of the protein and forms H-bonding with R553 and R557 of α5 region. On the other hand, due to the rearrangement of the C-terminus in two mutants, terminal oxygen of L632 form H-bonding with K610 in β4 region. (see Figure 4) Non-native H-bonding between C-terminus and K610 disrupts β2-β3-β4 regions in both mutants. As a result, the β–sheet contents in β2-β3-β4 regions of two mutants are lower than that of wtFAS1.
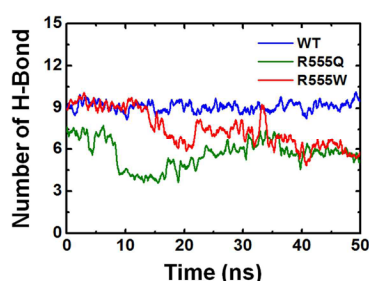
Figure 5. The number of hydrogen bonding in β2-β3-β4 regions of (a) wtFAS1, (b) R555Q, and (c) R555W.

Enhanced the degrees of hydrophobicity

We calculated the 3D-RISM theory to investigate the changes of thermodynamic properties upon the mutation. We decomposed the changes of solvation free energy, $\Delta\Delta\mu$ ($\Delta\Delta\mu = \Delta\mu_{mu} - \Delta\mu_{wt}$, that of the mutant ($\Delta\mu_{mu}$) and that of the wild type ($\Delta\mu_{wt}$)), into different regions of the proteins. As shown in Table 1, the solvation free energy for β2-β3-β4 regions is increased 53.85 kcal/mol and 115.24 kcal/mol in R555Q and R555W with respect to the wtFAS1. This results come from the exposure of hydrophobic residues in β2-β3-β4 regions and the enhanced non-native H-bonding between the hydrophilic residues of β4 region and adjacent hydrophilic residues.

This is further verified with the result of SASA analysis. The ΔSASA of all hydrophobic residues for overall structures is decreased -58.55 Å^2 and -82.71 Å^2, while the ΔSASA for β2-β3-β4 regions is increased 72.68 Å^2 and 64.54 Å^2 in R555Q and R555W with respect to wtFAS1. This is because non-native H-bonding between side-chain of hydrophilic residues of β2-β3-β4 regions and adjacent hydrophilic residues contribute to increase the hydrophobicity in β2-β3-β4 regions of two mutants.

The hydrophilic residues that interact with K610 are contributors for inducing the hydrophobic residues more exposed to solvent. Since the solvent-exposed hydrophobic residues are not favorable to be, they would try to assemble themselves to become more stable. This tendency, increasing the degrees of hydrophobicity of $\beta 2$-$\beta 3$-$\beta 4$ regions in the case of mutants, may arise to promote protein aggregation.

Conclusion

We represent *in silico* studies on the structural and thermodynamic characteristics of wtFAS1 and its two mutants, R555Q and R555W, related to corneal dystrophy. Mutation effects were also studied to examine whether the structural and thermodynamic features that we observe are responsible for the aggregation potential. We focused on the two mutants because they are well-known mutants[11] but have unknown aggregation propensity[13,16,25]. We find that the protein dysfunction due to the rearrangement of C-terminus caused by enhanced hydrophobic contacts and increased solvation free energy of $\beta 2$-$\beta 3$-$\beta 4$ region upon the non-native H-bonding. These features are mutation-dependent, and partially experimentally measured, it is suggested that (i) enhanced hydrophobic interactions of mutation site, (ii) rearrangement of C-terminus, (iii) protein dysfunction due to the blockage of YH motif, and (iv) increased solvation free energy of $\beta 2$-$\beta 3$-$\beta 4$ region, are the structural and thermodynamic characteristics of two mutants that affect aggregation prone potential. We believe that our results provide to reveal the structural and thermodynamic information of protein aggregation.

Acknowledgments

References

1. Skonier, J.; Neubauer, M.; Madisen, L.; Bennett, K.; Plowman, G. D. ; Purchio, A. F. DNA Cell. Biol. 1992, 11, 511.

2. Klintworth, G. K.; Enghild J. J.; Valnickova Z. Invest. Ophthalmol. Vis. Sci 1994, 5, 1938.

3. LeBaron, R. G.; Bezverkov, K. I.; Zimber, M. P.; Pavelec, R.; Skonier, J.; Purchio, A. F. J. Invest. Dermatol. 1995, 104, 844.

4. Kitahama, S.; Gibson, M. A.; Hatzinikolas, G.; Hay, S.; Kuliwaba, J. L.; Evdokiou, A.; Atkins, G. J.; Findlay, D. M. Bone 2000, 27, 61.

5. Lee, S. H.; Bae, J. S.; Park, S. H.; Lee, B. H.; Park, R. W.; Choi, J. Y.; Park, J. Y.; Ha, S. W.; Kim, Y L.; Kwon, T. H.; Kim, I. S. Kidney Int. 2003, 64, 1012.

6. Billings, P. C.; Whitbeck, J. C.; Adams, C. S.; Abrams, W. R.; Cohen, A. J.; Engelsberg, B. N.; Howard, P. S.; Rosenbloom, J. J. Biol. Chem. 2002, 277, 28003.

7. Hashimoto, K.; Noshiro, M.; Ohno, S.; Kawamoto, T.; Satakeda, H.; Akagawa, Y.; Nakashima, K.; Okimura, A.; Ishida, H.; Okamoto, T.; Pan, H.; Shen, M.; Yan, W.; Kato, Y. Biochim. Biophys. Acta. 1997, 1355, 303.

8. Bae, J. S.; Lee, S. H.; Kim, J. E.; Choi, J. Y.; Park, R. W.; Park, H. S.; Sohn, Y. S.; Lee, D. S.; Lee, E. B.; Kim, I. S. Biochem. Biophys. Res. Commun. 2002, 45, 940.

9. Skonier, J.; Bennett, K.; Rothwell, V.; Kosowski, S.; Plowman, G.; Wallace, P.; Edelhoff, S.; Disteche, C.; Neubauer, M.; Marquardt, H.; Rodgers, J.; Purchio, A. F. DNA Cell. Biol. 1994, 13, 571.

10. Kim, J. E.; Kim, S. J.; Jeon, H. W.; Lee, B. H.; Coi, J. Y.; Park, R. W.; Park, J. Y.; Kim, I. S. Oncogene 2003, 22, 2045.

11. Knnabiran, C.; Klintworth, G. K. Hum. Mutat. 2006, 7, 615.

12. Munier, F. L.; Frueh, B. E.; Othenin-Girard, P.; Uffer, S.; Cousin, P.; Wang, M. X.; Heon, E.; Black, G. C. M.; Blasi, M. A.; Balestrazzi, E.; Lorenz, B.; Escoto, R.; Barraquer, R.; Hoeltzenbein, M.; Bloor, B.; Fossarello, M.; Singh, A. D.; Arsenijevic, Y.; Zografos, L.; Schorderet, D. F. Invest. Ophthalmol. Vis. Sci. 2002, 43, 949.

13. Underhaug, J.; Koldso, H.; Runager, K.; Nielson, J. T.; Sorensen, C. S.; Kristensen, T.; Otzen, D. E.; Karring, H.; Malmendal, A.; Schiott, B.; Biochim. Biophys. Acta. 2013, 1834, 2812.

14. Clout, N. J.; Tisi, D.; Hohenester, E. Structure 2003, 11, 197.

15. Clout, N. J.; Hohenester, E. Mol. Vis. 2003, 9, 440.

16. Thapa, N.; Lee, B-H.; Kim, I-S. Int. J. Biochem. Cell Biol. 2010, 42, 39.

17. Case, D. A.; Darden, T. A.; Cheatam, T. E., III; Simmerling, C. L.; Wang, J.; Duke, R. E.; Luo, R.; Merz, K. M.; Pearlman, D. A.; Crowley, M.; Walker, R. C.; Zhang, W.; Wang, B.; Hayik, S.; Roitberg, A.; Seabra, G.; Wong, K. F.; Paesani, F.; Wu, X.; Brozell, S.; Tsui, V.; Gohlke, H.; Yang, L.; Tan, C.; Mongan, J.; Hornak, V.; Cui, G.; Beroza, P.; Mathews, D. H.; Schafmeister, C.; Ross, W. S.; Kollman, P. A. AMBER 9. University of California: San Francisco, 2006.

18. Hornak, V.; Abel, R.; Okur, A.; Strockbine, B.; Roitberg, A.; Simmerling, C. Proteins 2006, 65, 712.

19. Jorgensen, W. L.; Chandrasekhar, J.; Madura, J. D.; Impey, R. W.; Klein, M. L. J. Chem. Phys. 1983, 79, 926.

20. Guex, N.; Peitsch, M. C. Electrophoresis 1997, 18, 2714.

21. Darden, T.; York, D.; Pedersen, L. J. Chem. Phys 1993, 98, 10089.

22. Ryckaert, J. P.; Ciccotti, G.; Berendsen, H. J. C. J. Comput. Phys. 1977, 23, 327.

23. Kovalenko, A. In Molecular Theory of Solvation; Hirata, F., Ed.; Kluwer: Dordrecht, Netherlands, 2003; p. 169.

24. Imai, T.; Harano, Y.; Kinoshita, M.; Kovalenko, A.; Hirata, F. J. Chem. Phys. 2006, 125, 024911.

25. Runager, K.; Basaiawmoit, R.V.; Deva, T.; Andreasen, M.; Valnickova, Z.; Soresen. C. S.; Karring, H.; Thogersen, I. B.; Christiansen, G.; Underhaug, J.; Kristensen, T.; Nielsen, N. C.; Klintworth, G. K.; Otzen, D. E.; Enghild, J. J. J. Biol. Chem. 2011, 286, 4951

26. Ferguson, J.W.; Thoma, B. S.; Mikesh, M. F.; Kramer, R. H.; Bennett, K. L.; Purchio, A; Bellard, B. J.; LeBaron R. G. Cell Tissue Res. 2003, 313, 93.

27. Kim, M. O.; Yun, S. J.; Kim, I. S.; Sohn, S.; Lee, E. H. Neurosci. Lett. 2003, 336, 93.

28. Nam, J. O.; Jeong, H. W.; Lee, B. H.; Park, R. W.; Kim, I. S. Cancer Res. 2005, 65, 4153.

29. Kim, J. E., Jeong, H. W., Nam, J. O., Lee, B. H., Choi, J. Y., Park, R. W.; Park, J. Y.; Kim, I. S. J. Biol. Chem. 2002, 277, 46159

30. Kim, J. E.; Kim, S. J.; Lee, B. H.; Park, R.W.; Kim, K. S.; Kim, I. S. J. Biol. Chem. 2000, 275, 30907